Review Article

Potluri Anudeep, M. Achyutha Kumar Reddy, Veerendrakumar C. Khed, Musa Adamu*, Mada Varalakshmi, Yasser E. Ibrahim, and Omar Shabbir Ahmed

Effect of superplasticizer in geopolymer and alkali-activated cement mortar/concrete: A review

https://doi.org/10.1515/rams-2023-0173 received October 16, 2023; accepted December 26, 2023

Abstract: The cement and construction industry creates around 10% of the global carbon footprint. Geopolymer and alkali-activated concrete provide a sustainable solution to conventional concrete. Due to its disadvantages, the practical usage of geopolymer and alkali-activated concrete is limited. Workability is one of the issues faced in developing geopolymer and alkali-activated concretes. Plenty of research was conducted to provide a solution to enhance the ability to use different superplasticizers (SPs). The present article extensively reviews the effects of SPs on geopolymer and alkali-activated concretes. The research articles published in the last 5 years in high-quality journals are considered for the chemical composition of the different SPs and analyses of their exact impact on geopolymer and alkali-activated cement mortar and concrete. Later, the impact of SPs on the normal consistency and setting times of cement mortar, workability, compressive strength, flexural strength, split tensile strength, microstructure, and water absorption of geopolymer and alkali-activated concrete was determined. SPs improve the geopolymer and alkali-activated concretes upon their use in desired dosages; more dosage leads to negative effects. Therefore, selecting the optimal superplasticizer is essential since it impacts the performance of the geopolymer and alkali-activated concrete.

Keywords: geopolymer concrete, superplasticizer, rheological properties

1 Introduction

Over the decades, cement has been the most used material in construction. Manufacturing cement involves a large quantity of raw materials and energy. During the production of clinker, the raw materials are heated at high temperatures, resulting in the emission of carbon dioxide (CO₂) [1]. There is a need to reduce the energy and CO₂ emitted from the cement manufacturing industry [2-6]. The introduction of pozzolanic materials as substitutes to reduce clinker utilization in cement was initiated around four decades [7-9]. Pozzolanic materials are the byproducts from the industries, exhibiting rich SiO₂ content [10-12]. In practical usages, the pozzolanic material utilization was limited to less than 40% [13], which does not result in the reduction of more carbon footprint. Due to the availability of SiO₂ and Al₂O₃ contents in suitable percentages, the total utilization of pozzolanic material as a binder is possible in the case of its use as source materials in geopolymer concrete [13–15].

The geopolymer concrete was introduced in the early 1980s; it enabled an opportunity to utilize the pozzolanic materials to their maximum percentage [16–19]. Geopolymer is an inorganic polymer produced from alkali-activated pozzolanic materials that contain SiO_2 and $\mathrm{Al}_2\mathrm{O}_3$ as the prime components (aluminosilicate materials) activated by alkaline solutions [20–25]. The aluminosilicate source materials [26–28] include fly ash, blast furnace slag, and geological-originated materials such as metakaolin [29,30]. Most of these raw materials are wastes from industries and thermal power plants [31–33]. Generally, mixtures of sodium hydroxide solution (NaOH) and sodium silicate solution (Na₂SiO₃) with various Na₂SiO₃/NaOH [34–36] mass ratios are most widely used as alkaline

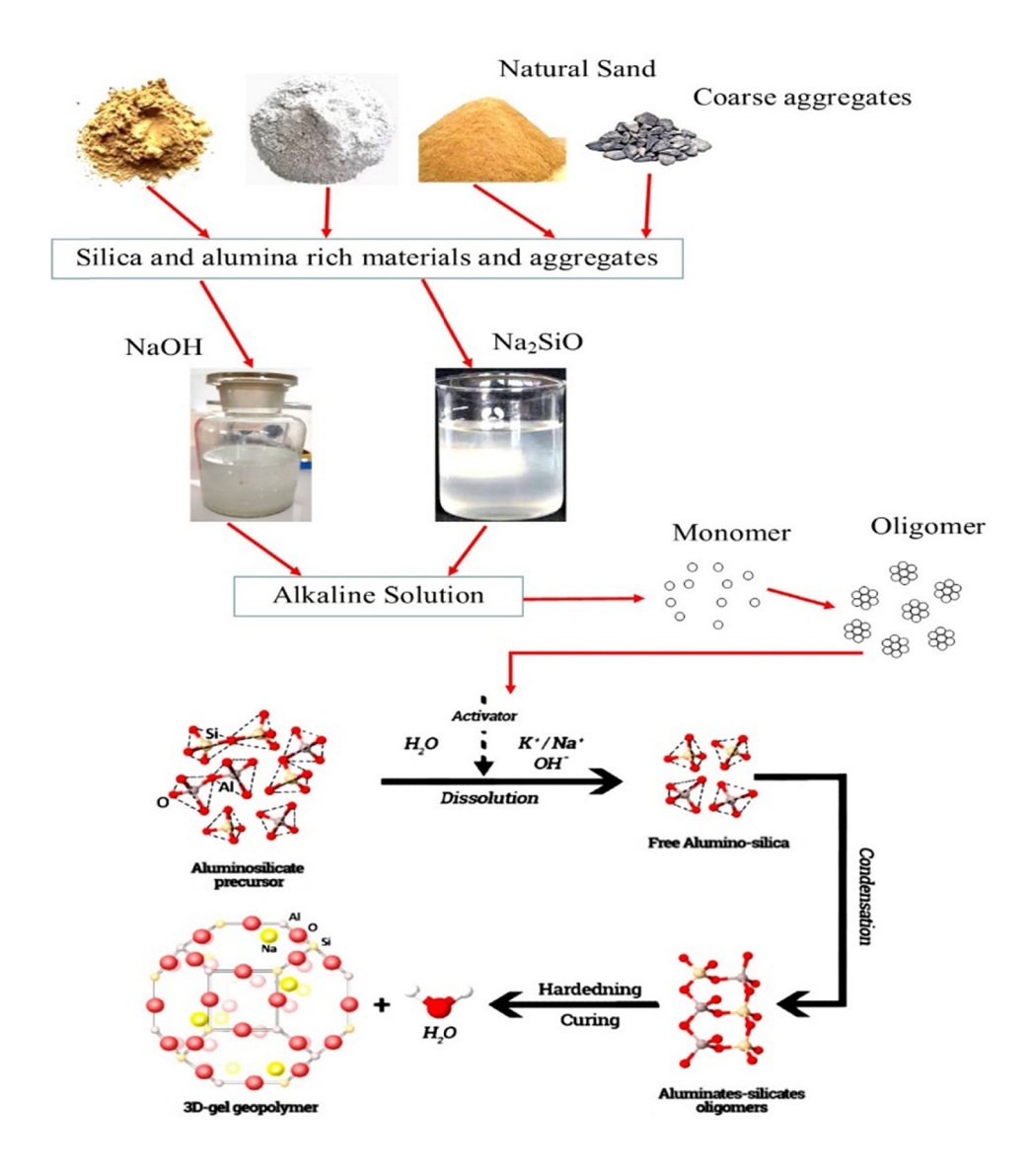
Potluri Anudeep, M. Achyutha Kumar Reddy, Mada Varalakshmi: Department of Civil Engineering, Koneru Lakshmaiah Education Foundation, Guntur, Vaddeswaram, India

Veerendrakumar C. Khed: Department of Civil Engineering, KLE Technological University DR. M.S. Sheshgiri Campus, Udyambag, Belagavi, Karnataka, 590008, India

Yasser E. Ibrahim, Omar Shabbir Ahmed: Engineering Management Department, College of Engineering, Prince Sultan University, 11586, Riyadh, Saudi Arabia

^{*} Corresponding author: Musa Adamu, Engineering Management Department, College of Engineering, Prince Sultan University, 11586, Riyadh, Saudi Arabia, e-mail: madamu@psu.edu.sa

2 — Potluri Anudeep et al. DE GRUYTER



Geopolymer mechanism and process

Figure 1: Geopolymer mechanism and process [39].

activators [37]. Calcium in source material leads to calcium–silicate–hydrate (C–S–H) gel when a moderately alkaline solution activates blast furnace slag. In contrast, calcium aluminosilicate hydrate (C–A–S–H) gels are created when high calcium-content aluminosilicates are activated [38]. The activation of low calcium aluminosilicates will form the N–A–S–H gels. The alkaline liquids such as sodium silicate and sodium hydroxide come in contact with alumina and silica-rich materials then Si and Al atoms present in the alumina and silica-rich materials dissolve in alkaline liquids, then a gel-type structure is formed, binding the aggregates and any other unreacted constituents of the concrete together to

produce a new material called geopolymer concrete, displayed in Figure 1 [39]. The chemical process in the geopolymerization activity is essentially Si and Al atoms will get dissolved in the OH⁻ solution from sodium hydroxide and reorients itself and sets as inorganic polymer under the process of polycondensation. Polycondensation is the process of forming polymers by the combination of different monomers; this process is frequently accompanied by the release of various subsidiary low-molecular products [40]. The difference between polymerization and polycondensation is that in polymerization process, the composition of the monomer and polymer is identical and in the polycondensation process, the composition of the final

macromolecule may significantly differ from the original composition of the monomer [41–51].

Geopolymer and alkali-activated concrete production consumes lower energy and emits reduces the embodied carbon footprint. The percentage reduction in carbon footprint can range from 30 to 80% or more, which depends on the raw materials and specific formulations used based on the specific mix designs, production processes, and regional factors. About 410 kg·m⁻³ carbon is emitted for the manufacture of structural concrete, and 242.87 kg·m⁻³ of carbon is emitted to produce geopolymer concrete. The percentage of reduction of carbon footprint by replacing conventional concrete with geopolymer and alkali-activated concrete is almost 60% [52-54]. It was proved that using geopolymer concrete would significantly reduce the carbon footprint without compromising the strength and durability properties compared with OPC concrete [55-57]. Geopolymer concrete still needs to be used in the construction industry; one of the reasons behind that is its complex rheological properties. Geopolymers based on fly ash possess stiffness and reduce the workability of the concrete [58]. Calcium content in the fly ash significantly impacted the geopolymer concrete [59]. The use of blends in the preparation of concrete has drawbacks in terms of reducing the properties, shrinkage, delay in hardening, and low performance of concrete, and also that concentration of alkaline solution affects the workability of geopolymer concrete [60]. Therefore, different chemical admixtures are widely used in geopolymer concrete to enhance its rheological properties; they have diverse effects [61].

Superplasticizer is a type of high-range water reduction admixture; the main objective is to improve the rheological performance of concrete. Adding a superplasticizer will majorly result in improved workability properties, and strength and durability can also be enhanced [33,60,62,63]. Some of the superplasticizers (SPs) that are used in geopolymer concrete include polycarboxylates, polycarboxylate ether (PCE), naphthalene, lignosulfonates, melamine, sulfonated melamine formaldehyde (SMF), and sulfonated naphthalene formaldehyde (SNF). Among all the SPs, SNF and PCE are widely used in India.

It is worth noting that the selection and dosage of SPs should be carefully considered based on the specific concrete mix design [64], environmental conditions, and project requirements to achieve the desired results [65]. SPs are commonly used in the construction industry for various applications, including high-strength concrete, self-compacting concrete, precast concrete, and ready-mix concrete. They are typically used when achieving higher strength while maintaining good workability and durability [66-71].

Limited standardization of codes, longer setting time, variability in raw materials, initial cost, availability of raw materials, and limited industry familiarity are the key disadvantages of geopolymer and alkali-activated concrete [15,72]. Lesser setting time and compatibility with admixtures are the common challenges faced in the development of geopolymer and alkali-activated concretes; it results in construction delays. The use of SPs in geopolymer and alkali-activated concrete leads to cost savings by optimizing the mix design. SPs are commonly used in conventional concrete as well. The cost implications here would depend on the specific formulation and dosage needed to achieve the desired properties [73-75]. The utilization of SPs in the concrete is given a boost in strength and durability by adding high range water reducing admixtures to reduce water content while maintaining constant workability. Each type of superplasticizer has different effects on the geopolymer concrete.

This article studies the effects of SPs on the geopolymers' rheological, strength, and durability properties and the alkali-activated materials. This study provides knowledge on the utilization of SPs in geopolymer concrete. This article studied and discussed various aspects of geopolymer concrete properties.

2 Methodology

The main goal of this review is to present the performance of SPs in geopolymer concrete. Initially, the literature was collected from Science Direct, Google Scholar, and Research Gate Science Hub. The publications were collected using the keywords "geopolymers," "alkali-activated materials," "SPs," and "replacement materials." In the beginning, the collected literature helped identify various available alternative materials for replacement in concrete. Furthermore, the gathered papers were refined utilizing the keywords fly ash, GGBS, metakaolin, nanoclay, and ferronickel slag (FS) as the substitution materials and naphthalene, PC, melamine, lignosulfonate as SPs. Afterwards, the following examination questions were outlined to get exceptionally significant exploration articles to the current review.

- a) What are SPs used in geopolymer concrete?
- b) Whether the properties of all SPs are similar or not?
- c) Has the superplasticizer shown any impact on the rheological properties of geopolymer concrete?
- d) What are superplasticizer's influences on geopolymer concrete's strength and durability?
- e) Do the SPs used in this study improve the geopolymer concrete properties?

Figure 2 gives information on the number of publications in different years. The last six years' publication data are taken for journals such as *Cement and Concrete Research*, *Cement and Concrete Composites*, and *Journal of Clear Productions*. Considering these data is taken at the starting stage of my research, we can identify that the *Journal of Clear Production* has more papers in my research area. We can observe that the investigation has been increasing gradually in the past 2 years in *Cement and Concrete Composites*. In the three journals, *Cement and Concrete Research*, *Cement and Concrete Composites*, and *Journal of Clear Production* in the plot, we can identify that the *Journal of Clear Production* has had more papers for the past 5 years, and in 2021 year, most articles were published including all three considered.

Identifying the different properties of pozzolanic materials helps to identify the fresh and hardened characteristics of the concrete. The prime materials used in geopolymer concrete are waste materials, which can have high viscosity and low workability. Several researchers studied the properties of concrete made using by-products generated through industries such as fly ash and GGBS [76] under varying conditions. Initializing SPs' physical and chemical characteristics is the first step in determining the potential risks in alkali-activated concrete. Under various circumstances, several researchers investigated the characteristics of concrete made using industrial products, including fly ash and GGBS. SPs have several critical characteristics crucial to understanding, including their chemical composition, molecular structure, dosage, compatibility with other materials, and impact on the characteristics of concrete.

3 Chemical admixtures

Generally, studying the superplasticizer's characteristics is essential for creating new and better formulations that can meet the rising demands of modern construction practices, improving the durability and quality of concrete. Strength, workability, and durability are facilitated by understanding the qualities. Various superplasticizer groups are available: naphthalene-based SPs, poly-carboxylic-based SPs, SMF, and SNF [77]. One was a modified naphthalene sulfonate SP known by the commercial name DARA-CEM and is referred to as naphthalene-based naphthalene (NP). The other was a PC-based SP known by the commercial name ADVA Cast 555 and referred to here by PC. The physical and chemical properties of the SPs are given in Table 1 [33,60,78–80].

Chemical admixtures are specialized additives added to concrete mixtures to modify their properties during mixing, placing, and curing. These admixtures can influence the workability, setting time, strength development, durability, and other performance aspects of concrete. They enhance concrete's overall quality and functionality in various construction applications.

SPs improve the workability of geopolymer concrete without significantly increasing the water content. This enhanced workability allows for better dispersion of the geopolymer binder and aggregates, improving strength due to better interfacial bonding. The reduced water content also contributes to denser and more impermeable concrete, which enhances durability by reducing porosity and permeability [81].

4 Properties of concrete

4.1 Rheological properties of concrete

Concrete is a complex material with distinct rheological properties due to its particulate nature and cementitious

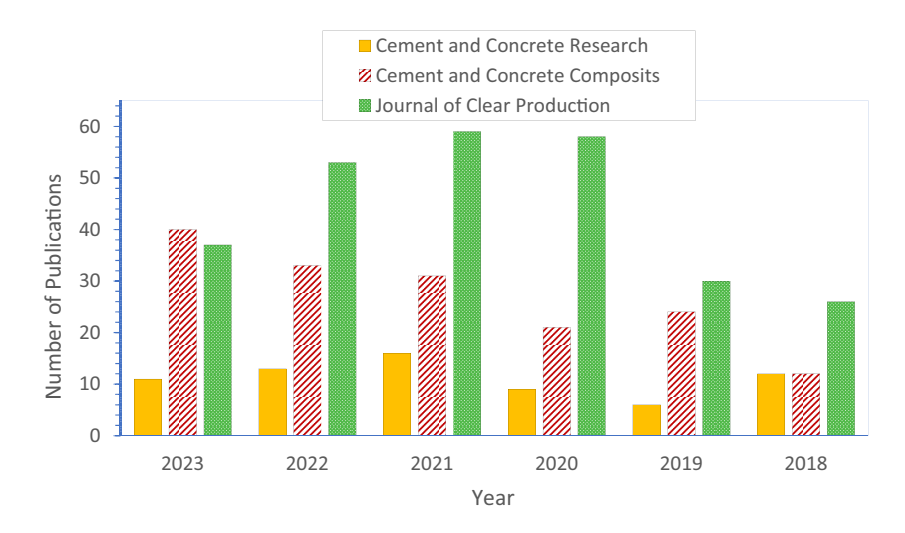


Figure 2: Number of publications for different journals.

Table 1: Physical and chemical properties of the SPs

SP	Total solids (%)	Specific gravity	pH value	Ref.
ADVA (PC)	39.2-40.8	1.08-1.09	4.8-6.8	[58]
DARACEM (NP)	41.0-43.0	1.20-1.23	6.0-9.0	[58]
Melamine formaldehyde	40	_	8.22	[82]
Naphthalene formaldehyde	40	_	7.86	[82]
Vinyl copolymer	25	_	6.80	[82]
Polycarboxylate admixtures (PC1)	38	_	5.40	[83]
Polycarboxylate admixtures (PC2)	38	_	4.65	[83]
Melamine	40	_	8.22	[83]
Naphthalene based	40	_	7.86	[83]
Vinyl copolymer	25	_	6.80	[83]
Polypropylene glycol derivative	_	_	10.70	[83]
Naphthalene-based SP	23	_	_	[84]
PCE1, PCE2, PCE3	30	_	_	[60]
ME	40	_	_	[60]
VC	25	_	_	[60]
SMF	42.40	1.26	9.03	[33]
Naphthalene formaldehyde	41.10	1.24	7.49	[33]
PCE	38.7	1.1	7.05	[33]
Naphthalene-based	_	_	8.0 ± 1	[85]
Polycarboxylate-based	_	_	6.5 ± 1	[85]
Naphthalene formaldehyde polymers	_	_	_	[61]
Polycarboxylate (PC1, PC2, PC3)	_	_	5.0 ± 1	[86]
Naphthalene based (N1, N2)	_	_	7.0 ± 0.5	[86]

binders. The rheological behavior of concrete is essential for its placement, consolidation, and curing during construction [87-94].

4.1.1 Setting time

Setting time is the amount of time needed for the paste to solidify. The paste comprises the source material and an alkaline solution [95]. The setting is caused mainly when the SiO₂ and Al₂O₃ particles react with an alkaline solution. The initial setting time of geopolymer concrete binders with or without white soil substitution is about 52.5-105 min, while the final setting time is between 180 and 225 min [71,96,97]. SMF and SNF SPs typically exhibit a moderate retarding effect on setting times. They can extend the time before the concrete begins to harden. PCE-based SPs are known for their ability to effectively reduce water content without significantly retarding setting times. The setting time can be influenced by the dosage of the superplasticizer. Higher dosages of certain types of SPs, particularly SMF and SNF, may lead to more significant retardation. Ambient temperature can also impact setting times. Warmer temperatures generally accelerate the setting, while colder temperatures may slow it down. The alkali content in geopolymer and alkali-activated concrete can affect setting times. Higher alkali concentrations may contribute to faster setting [71,98-103].

The first bars in Figure 3 display the initial setting time for 10% GGBS and 8% OPC. The setting rate depends on the type of additives, and it will be accelerated with increased calcium content. For the additives, the initial setting time for 10% GGBS with 90% fly ash is 203, and the initial setting time for 8% OPC with 92% fly ash is 110. The setting time decreases with the decrease in fly ash content because the setting time depends on the type of additives added to the mix and is accelerated with the increase of calcium content in the additives [29]. The second set of bars in Figure 3 shows that the mix uses 20% GGBS, 30% GGBS, and 35% alkaline activators. We can observe from the graph that when the slag content is increased in the mix, the initial setting time is reduced. When 20% of GGBS is used, the initial setting is 100; when 30% of GGBS is used, the initial setting time is 40. It supports that the higher the slag content in the past, the lesser the setting time is. This is because the heat of hydration for slag is more than fly ash, and when 35% of an alkaline activator is used, the initial setting time is increased because of the low heat of hydration in an alkaline solution [24].

The third set of bars is shown in Figure 3, CHN-3-P CHN-5-P CHN-7-P CHN-9-P, in which CH is Ca(OH)2; N is Na₂CO₃; P is paste; 3, 5, 7, and 9 are Na₂O equivalents.

6 — Potluri Anudeep et al. DE GRUYTER

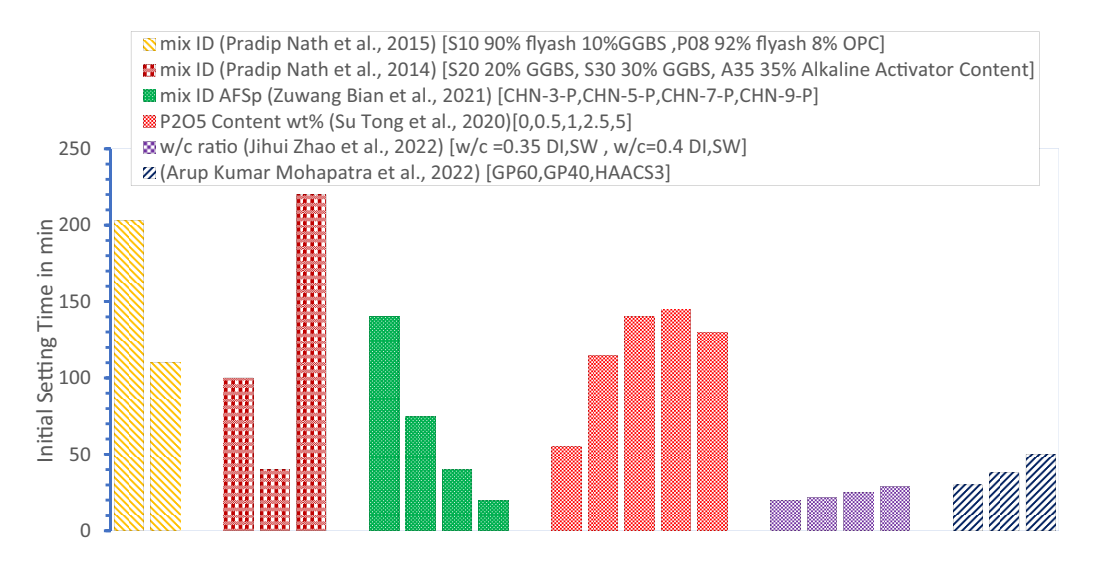


Figure 3: Initial setting time for different mix proportions.

The setting time of AFSP is decreased upon the rise of Na_2O equivalent because of the high volume of sodium oxide. The setting time is reduced if sodium oxide is more in volume. The bond formation is rapid and fast [104]. The fourth set of bars in Figure 3 displays P_2O_5 content in weights of 0, 0.5, 1, 2.5, and 5%. An increment in the initial setting time was observed upon of P_2O_5 to certain content and a decrease in initial setting time after 2.5% of P_2O_5 content. This can be attributed to the P_2O_5 increase in the initial setting time for less content. For more content of P_2O_5 , setting time decreases, which means for more content of P_2O_5 , there is a reduction in initial setting time, so more content of P_2O_5 heat of hydration is reduced in setting time [3].

The fifth set of bars in Figure 3 displays the initial setting time of W/C = 0.35 and W/C = 0.4 for deionized (DI) and salt water (SW) is presented in which DI and SW mean deionized water mixed alkali-activated slag and fresh paste of seawater mixed alkali-activated slag. The plot shows that the initial setting time of AAS improves with the increase of the W/C ratio, which means that the water content is more in increased W/C ratios, so it takes more time to set. For SW, the initial setting time is slightly slower than DI. This is because the hydration time is delayed to some extent in seawater, so the initial setting is more in seawater when compared to deionized water (heat of hydration is less in seawater) [105]. The sixth set of bars in Figure 3 displays the setting times for mixes GP60 (60% OPC), GP 40 (40% OPC) and Hybrid alkali activated cements (HAACS3). The reduction of OPC content led to increase in initial setting times due to the low heat of hydration resulting from the less cement content. Furthermore, for the HAACS3, the initial setting time also improves due to the low heat of hydration in the mix [106].

The final setting time mainly depends on concrete mix proportions and vibration [107,108]. The first set of the bars in Figure 4 displays the final setting time for 10% GGBS and 8% OPC. The setting rate depends on the category of additives and will be speeded with increased calcium content. The additive's final setting time for 10% GBS with 90% fly ash is 375, and for 8% OPC with 92% fly ash is 240. The setting time decreases with the decrease in flash content because the setting time depends on the type of additives added to the mix and is improved with the increase of calcium content in the additives [29]. The second set of bars in Figure 4 displays 20% GGBS, 30% GGBS, and 35% alkaline activators used in the mix. We can observe from the graph that when the slag content is increased in the mix, the final setting time is reduced. When 20% of GGBS is used, the initial setting is 100 min; when 30% of GGBS is used, the initial setting time is 40 s. It supports that the higher the percentage of the slag content in the paste, the lesser the setting time. It is because the heat of hydration for slag is more than flesh, and when 35% of the alkaline activator is used, the final setting time is increased because of the low heat of hydration in an alkaline solution [24].

The third set of bars in Figure 4 shows CHN-3-P CHN-5-P CHN-7-P CHN-9-P, in which CH is Ca(OH)₂; N is Na₂CO₃; P is paste; 3, 5, 7, and 9 are Na₂O equivalents. The setting time of AFSp decreases with the increase of Na₂O equivalent because of the high volume of sodium oxide. The setting time is reduced if sodium oxide is more in volume, and the bond formation is rapid and fast [104]. The fourth set of bars in Figure 4 shows P_2O_5 content in weight of 0, 0.5, 1, 2.5, and 5%. If P_2O_5 content increases, an increment was observed in the final setting time up to certain P_2O_5

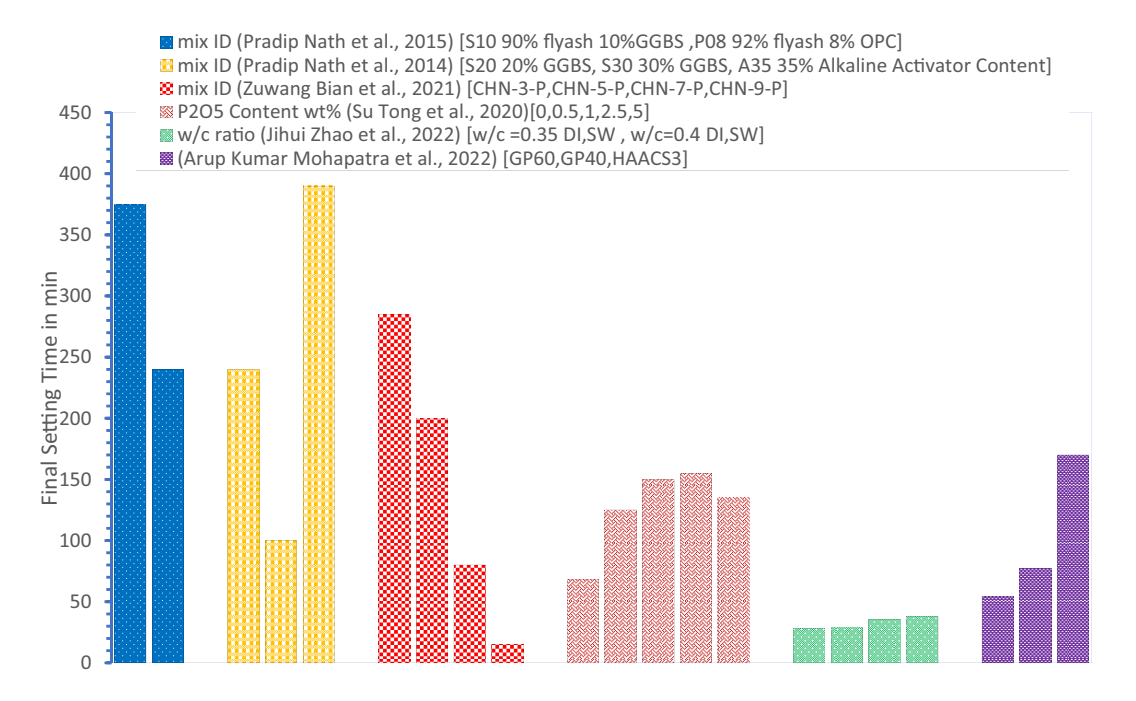


Figure 4: Final setting time for different mix proportions.

content and a decrease in final setting time after 2.5% of P_2O_5 content. This is because P_2O_5 increases the initial setting time for less content and decreases it for more content. This means that for more P_2O_5 , there was a decrease in the final setting time, which indicates that more P_2O_5 causes a greater reduction in setting time due to heat of hydration [3].

The fifth set of bars in Figure 4 displays the final setting time for W/C = 0.35 and W/C = 0.4 for DI and SW is presented in which DI and SW mean deionized water mixed alkali-activated slag and fresh paste of seawater mixed alkali-activated slag. The plot shows that the final setting time of AAS improves with the increase of W/C ratio, which means that the water content is more in increased W/C ratios, so it takes more time to set. For SW, the final setting time is slightly extended than DI. This is because the hydration time is delayed to some extent in seawater, so the initial setting is more in seawater when compared to deionized water (heat of hydration is less in seawater) [105]. The sixth set of bars in Figure 4 presents the final setting times for mixes GP60, GP40 and HAACS3. We can see that the reduction in OPC content increases the final setting time due to the lower heat of hydration resulting from lesser cement content. Considering HAACS3, due to its lower heat of hydration, its final setting time increases also [106].

4.1.2 Normal consistency

The normal consistency describes the water content required to achieve a specific consistency or standard degree of stiffness in a cement paste. This test is part of the initial phase of determining the optimal water-to-cement ratio for producing concrete with desired properties. Consistency of concrete increases as supplementary components are added, resulting in increased water demand [31]. A study found that standard consistency increased by 1.6–3.1% when fly ash replaced 30–50% of OPC. Geopolymer concrete without superplasticizer has higher consistency, and admixture comprising paste also has higher consistency than that of OPC paste [109].

4.1.3 Workability

Workability is the volume of suitable internal work required to create full compaction [96]. In geopolymer concrete, workability also depends on an alkaline solution. The first bars in Figure 5 show the slump values of groups such as A-3, B-2, C-4, D-3, and E-3. Groups A and B display different proportions of materials used with sodium silicate compound alkaline activator, whereas silicate fume activator was utilized in C & D groups. It was observed that there is an improvement in the slump values for the A and B groups comparatively with the D and E groups; group C exhibited

better slump values among all groups. This may be attributed to the usage of more water content as well as mixing time in group C than in the remaining groups. It was already a fact that the slump depends mainly on water content and time of mixing. It also depends on the use of SPs [97]. The second set of bars in Figure 5 shows slump values of group S6 means proportions (kg·m⁻³) of UGGBS-250.6, FA(%)-107.4, SH-10, SP(%)-0.5, SP-SN, w/s-0.4, G-2 are taken in mix proportions, and slump is considered for different duration. In the S6 group, the plot shows a decrease in a slump for an increase in duration, which means that when duration increases, the slump decreases. As time increases, the setting starts, so the slump is low as time passes [30].

The third set of bars in Figure 5 displays the slump values for different durations of 30, 60, and 90 min and AAS1, AAS2, and OPC. Slag activated by powdered sodium silicate and lime slurry (AAS1) and slag activated by liquid sodium silicate and lime slurry (AAS2). The slump is more for AAS1 than others. This is because of the further dissolution of the powdered sodium silicate into mixing water. If fine particles are more, the workability will be greater because it takes more time to set; if fine particles are more, it takes more time to react [110]. The fourth set of bars in Figure 5 shows the slump values for different mix proportions: A15, B20, C25, and D25 combinations. A15 is for 85% FA and 15% GGBS, B20 is for 80% FA, and 20% GGBS; C25 is for 75% FA and 25% GGBS; and D25 is for 75% FA and 25% GGBS, with various alkaline activator binder ratios. A, B, C, and B ratios are 0.4, 0.4, 0.35, and 0.4, respectively. The alkaline activator binder ratio effect on workability is seen in different mixtures for different slag proportions. The difference in a slump is because of the different proportions

used in the mix [111]. The fifth set of bars in Figure 5 shows the slump values for different durations, such as 15, 10, 25, and 30 min and compound activator and compound activator + water reducing set retarding admixture (WRRe). As time passes, the slump reduces, and when compound activator alone is used, the slump is less, and when compound activator + WRRe is used, the slump is more. This means that when WRRs are used, workability increases, so the slump is greater [61]. In summary, the rheological properties are very important because if the mix exhibits good rheological properties, there will be a controlled setting of mix and better dispersion of paste and aggregates. This aims to find the optimum water content that can be used in the mix.

4.2 Strength properties of concrete

Concrete strength properties are critical indicators of its structural performance and durability. The strength of concrete is influenced by factors such as the mix design, water—cement ratio, curing conditions, aggregate properties, and any additional admixtures used.

4.2.1 Compressive strength

Concrete exploits its good compressive strength. It is the strength of concrete under compressive loading. It depends mainly on bond formation and many other factors such as proper curing, proper vibration of concrete, and mix proportions [96,112–117]. The first set of bars in Figure 6 shows

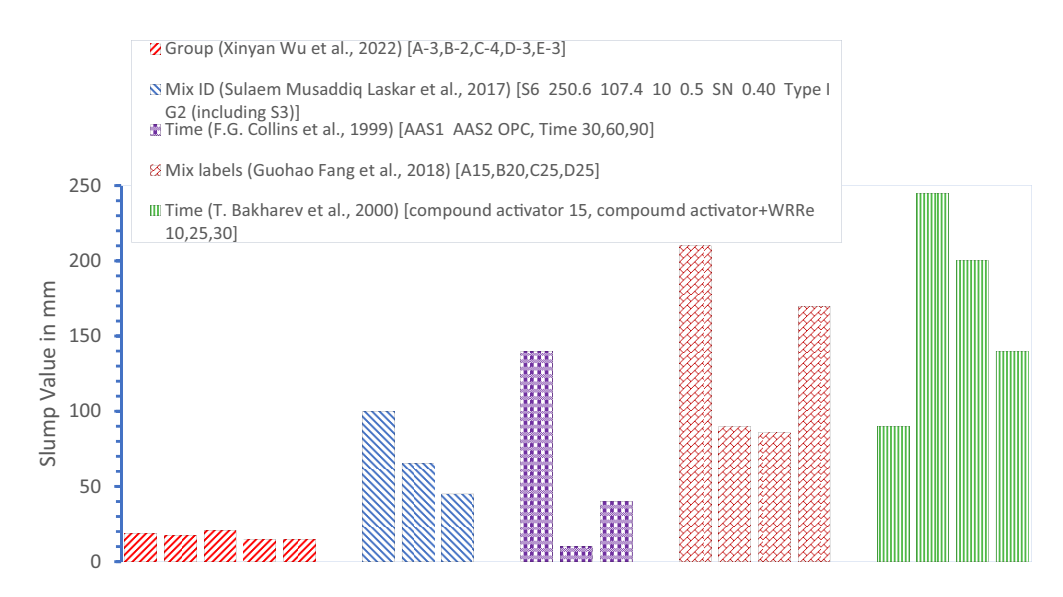


Figure 5: Slump values for different mix proportions.

compressive strength values for samples used by preparing F00 and S10. It means that F00 is 100% fly ash, and S10 is 90% fly ash and 10% GGBS. We can observe that samples made using 100% fly ash do not give any initial strength for 3 days. They give strength after 7 days. This is because flyash reacts slowly, so it gets compressive strength in later days. In samples with 10%, GGBS gives early-day strength. This is because GGBS reacts fast. The compressive strength also depends on the way of curing and proportions used in the mix [29].

The second set of bars in Figure 6 displays compressive strength values for different Na₂O equivalents (%), and for days 3 and 7, compressive strength increases for different proportions of mixes. We can observe that the first compressive strength increases with the increase in Na₂O equivalent (%), and a further increase in Na₂O equivalent (%) compressive strength decreases. This is due to the increase in Na₂O equivalent.

The rate of reaction and calcium aluminosilicate dissolution framework in the FNS is enhanced with the rise of the Na₂O equivalent, which results rich in calcium, silicon, and aluminum ions in the formation of reaction products which is responsible for the development of compressive strength. At low Na₂O equivalents, the inadequate dissolution of FNS in a moderately low reaction rate, thus hindering reaction product formation [104].

The third set of bars in Figure 6 displays the values for compressive strength for 0.5 N SPs. For different days in the plot, it can be observed that the compressive strength improves with an increase in days for different mix proportions. For 0.5 N superplasticizer, in which N means naphthalene superplasticizer, compressive strength increases with an increase in days or duration because the bond becomes stronger as time passes [3]. The fourth set of bars in Figure 6 shows the compressive strength values for various durations, such as 3 and 7 days, and for SW and DI mix samples, which indicate that the SW is a fresh paste of seawater mixed with alkali-activated slag and DI is for deionized water mixed alkali-activated slag.

An increment in the compressive strength was observed for DI samples comparatively with SW samples. It may be attributed to the weak in the formation of seawater bonds than deionized water. Furthermore, the addition of seawater will result in the decrement of compressive strength [105].

The fifth bar in Figure 6 shows the compressive strength values for different proportions, such as F1 and F2. Compressive strength gradually increases with the increase of time. We can identify that the compressive strength is greater for 3 and 7 days in F1 than in F2. It may be attributed to the fly ash utilization in the mix F2, which lowers reaction speed and resulted in the low compressive strength in initial days [118]. The sixth set of bars in Figure 6 displays the

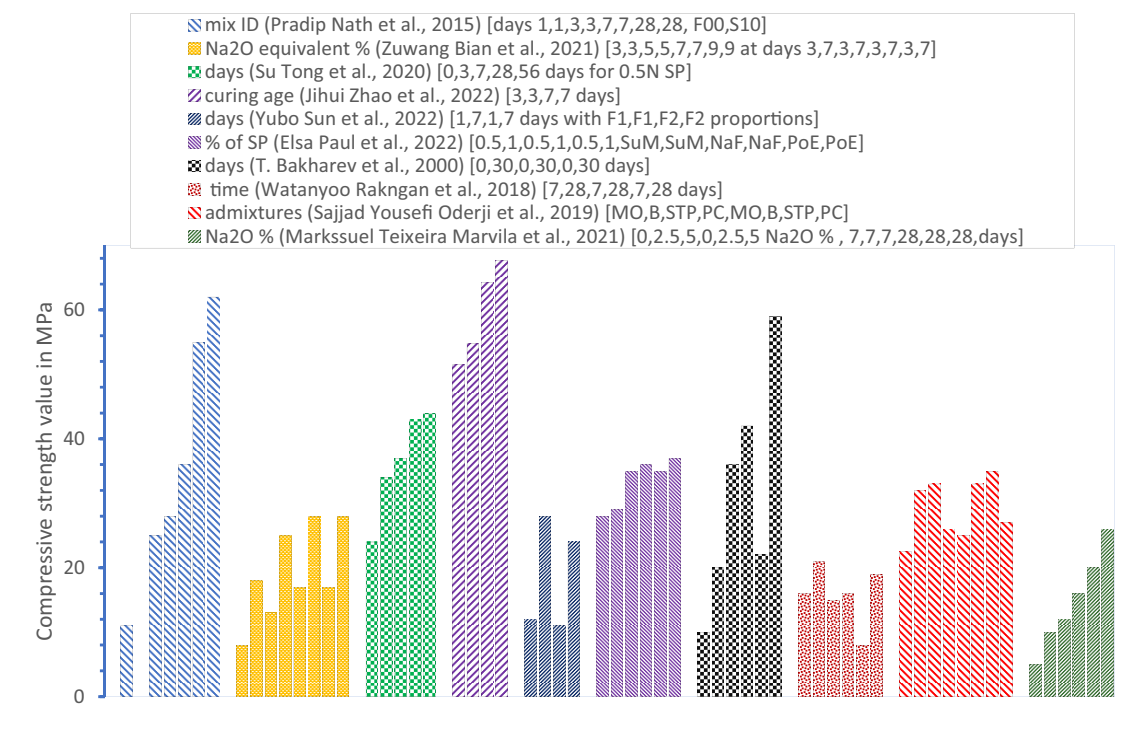


Figure 6: Compressive strength for different mix proportions.

compressive strength for various dosages (0.5 and 1) of SPs like sulfonated melamine formaldehyde (SMF), naphthalene formaldehyde (NaF), and carboxylate ether. It was observed that the SMF SPs show less compressive strength comparatively with others due to lower instability [33]. The seventh set of bars in Figure 6 shows compressive strength values for various days of 0 days and 30 days and different proportions of activators such as (compound activator 8% Na), (Na silicate, 4% Na), and (Na silicate, 7% Na + WRRe) are used compound activator 8% Na is having less compressive strength when relating to other this may be attributed to the compound activator as a mixture of sodium hydroxide (6.3% Na) and sodium carbonate (1.7% Na) two liquids are mixed in this compound activator. There might be bonding issues, so the compound activator does not produce high strength [61].

The eighth set of bars in Figure 6 displays the values of compressive strength for different days, 7 and 28 days; for different P, B, and R proportions of fly ash, we can observe that the compressive strength decreases for 7 days for different proportions of P, B, R; this is due to the soft texture of the test specimens during demolding and before determination of the compressive strength tests [119]. The ninth set of bars in Figure 6 shows the compressive strength values for various days, 7 days, and 28 days, and for different admixtures such as chemical admixtures are shown. Admixtures such as sodium tetraborate decahydrate-borax (B), sodium triphosphate (STP), and PC. If used, we can identify that the STP admixture shows more compressive strength than other admixtures. This is because of the more active participation of this admixture in alkali activation.

Compressive strength depends on mix proportions, curing, and bond formation when the alumina silica-rich source material reacts with an alkaline solution. Suppose that this process is good and bond formation is strong. In that case, the compressive strength is more so that the reaction between the aluminosilicate-rich materials and the alkaline solution is very important in getting compressive strength [120].

DE GRUYTER

The tenth set of bars in Figure 6 shows the compressive strength for different days, 7 days, and 28 days and for different Na_2O (%). We can observe that compressive strength increases with an increased Na_2O content, but this is for a certain increase only if Na_2O is further increased; there will be a loss of compressive strength. Compressive strength increases with an increase in duration or an increase in days. It is identified that the optimum content of sodium is 10%. Because of the level below 10%, the formation of a resistant phase is inadequate. Still above the 10% level, an electrical imbalance occurs, which drops in the strength, so sodium content should be up to 10% only [121].

4.2.2 Flexural strength

The ability to resist the bending of an unreinforced concrete beam or slab is referred to as the flexural strength of concrete [122–128]. Measured in modulus of rupture [96].

The first bars in Figure 7 show flexural strength for various 7- and 14-day duration and different proportions of sodium hydroxide 10, 12, 14, and 16 M. The plot shows that

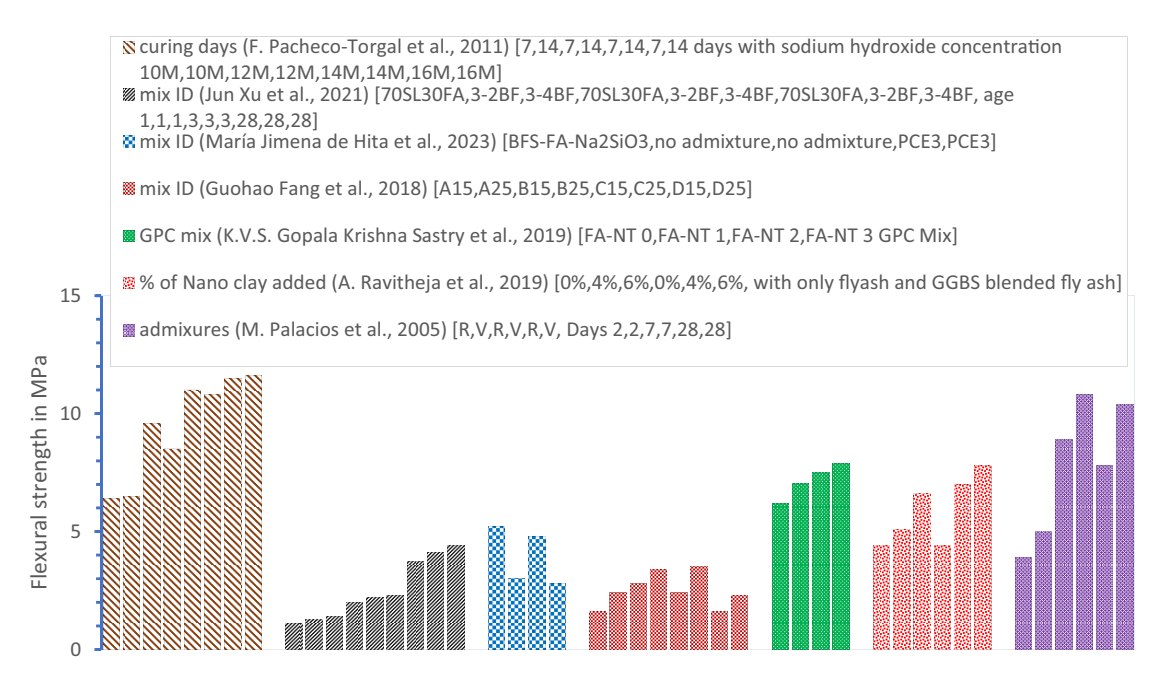


Figure 7: Flexural strength for different mix proportions.

flexural strength increases up to 7 days and a slight increase in flexural strength in specimens using 10 and 16 M of sodium hydroxide concentration. This depends on the proportions used in the mix and the binder material used. In both cases, the flexural strength improved with increment in sodium hydroxide concentration and superplasticizer content up to 3% blended with 10% calcium hydroxide content. These factors improved the peak levels of the mechanical strength by up to 90% [129].

The second set of bars in Figure 7 shows flexural strength for different proportions such as 70SL30FA, 3-2BF, and 3-4BF and for different durations 1, 3, and 28 days. It can be identified that the flexural strength increases with the increase in days. 70SL30FA means 70% slag and 30% fly ash. 3-2BF means 70% slag and 30% fly ash high calcium basalt fiber (HCBF) (%) is 2 and 3-4BF 70% slag and 30% fly ash HCBF (%) is 4. We can also observe that increased HCBF content increases flexural strength. This is because the used basalt has high calcium content, which helps improve the flexural content up to a certain limit [130]. The third set of bars in Figure 7 shows the flexural strength for 2 days and different proportions, such as BFS-FA-Na₂Co₃. We can observe that the initial flexural strength is less with the introduction of the PCE3 because of the SP introduction. So, with the introduction of a superplasticizer, the strength increases slowly. This flexural strength is low during the initial period [60]. The fourth set of bars in Figure 7 displays the flexural strength for different proportions such as A15, A25, B15, B25, C15, C25, D15, and D25, which means (85% FA 15% GGBS) (75% FA 25% GGBS). In the graph, we can observe that the percentage of GGBS increases in the flexural strength. Here, 28-day flexural strength is shown. In the case of an increase in the molarity of SH from 10 M (Series A) to 12 M (Series B), based on the Series A and Series C, an increment in the flexural strength of AAFS concrete was observed with the reduction of the AL/B ratio from 0.4 (Series A) to 0.35 (Series C). The effect of the SS/SH ratio on AAFS concrete's flexural strength was insignificant, as seen in Series A and Series D. The following phenomena are almost similar to the results shown in compressive strength development [111].

The fifth bar in Figure 7 shows flexural strength for different proportions, such as FA-NT0, FA-NT 1, FA-NT 2, and FA-NT 3. We can observe that the flexural strength increases with the increase in proportions (% of nano-Tio₂ added). This is because the nano-TiO₂ particle size is small, and the finer the particles, the more the compressive strength. So, an increase in the content of nano-TiO₂ increases flexural strength due to strong bond formation [131]. The sixth set of bars in Figure 7 shows flexural strength for different dosages of nanoclay for only fly ash and GGBS blended fly ash

for 28 days. We can identify that the GGBS blended fly ash consists of more flexural strength than only fly ash. This is because the proportions used are % of nanoclay of 0, 4, and 6. The flexural strength increases up to 6%. Flexural strength decreases if nanoclay content increases more than 6%. GGBS blended fly ash mix gives more flexural strength because GGBS bond formation is fast and strong compared to only fly ash mix [32]. The seventh set of bars in Figure 7 shows flexural strength for various durations of 2, 7, and 28 days and for different SPs R and V for the proportion of slag + water glass (4%Na₂O). It can be observed that the flexural strength increases with an increase in time. It also depends on the bond formation and the proportions used to prepare the mix, so optimum or suitable proportions are taken for good strength [83].

4.2.3 Split tensile strength

According to a study performed on GGBS, a water content of 14% and an SP dosage ranging from 2 to 6% by mass of the binder were used to create the five mixtures used in this study. As with compressive strength, the split tensile strength decreased with increased SP [132–134].

4.2.4 Microstructure of hardened concrete

The scanning electron microscopy (SEM) images of FS particles are illustrated in 1,000 × 5,000 magnification. The SEM images displayed that FS particles are unpredictable polygons with closed structures and flat cross-sections. SEM images generated from the intensity of backscattered electrons and the beam position can show the distribution of different elements in the sample. Heavier elements reflect more electrons and so will appear brighter in the image. SEM was applied to know the microstructure of AFS (alkali-activated FS). It can be observed that a large amount of gel phase on the face for the samples, identified as C-A-S-H gel of paste mixes, are made by the addition of 10 and 50% GGBFS to the total binder (slag and fly ash) to evaluate the microstructure of slag blended fly ash-based geopolymer, displayed in microstructural images of the samples at 28 days of age. The cement paste with 50% GGBFS is highly compact and lesser porous than that with 10% GGBFS. The poorly reacted and unreacted fly ash particles are most generally visible in the cement paste with 10% slag. In summary, strength properties mainly depend on the bond formation, mix proportions, and particle sizes. If the particle size is less, the gel formation is effective and possesses higher compressive strength. Curing

temperature and curing conditions are also very important for compressive strength – the durability of concrete or mortar increases when there are fewer pores, good bonding, and proper curing [135] (Figure 8).

4.3 Durability properties of concrete

The durability properties of concrete refer to its ability to resist deterioration and maintain its intended performance over time, especially when exposed to various environmental and service conditions. Ensuring the durability of concrete structures is crucial to extending their service life and minimizing maintenance and repair costs [73,136–140].

4.3.1 Water absorption

Water absorption is referred to as how much amount of water is absorbed by a material. It is calculated as the water absorbed to dry material's weight ratio. It depends on the pore structure of the concrete, material absorption capacity, and the nature of aggregates [141–143]. When the polymerization process happens consistently in elevated

temperatures during curing, it can provide more binding gel to fill water-filled pores, reducing water absorption [144–146]. The first bars in Figure 9 show water absorption for 28 and 56 days and different proportions. We can observe that in most cases, water absorption is decreased by an increase in days. This depends on the proportions used in the mix and the size of the particles. If the size of particles is finer, strength will be greater, and strength will gain gradually [12]. The second set of bars in Figure 9 shows water absorption for different proportions of silica content. We can observe that the water absorption decreases with the increase in silica content. Higher apparent porosity and water absorption are noted in silica, ranging from 1.6 to 4.8%. So, a decrease in water absorption is noted in a range of 1.6 to 4.8% of silica, with SiO₂ content of 6.4 and 8%, indicating that the incorporation of soluble silicates led to a denser and homogeneous microstructure [147].

The third set of bars in Figure 9 shows water absorption for different ratios of GBFS/(GBFS + MK) 1, 0.9, and 0.8 and S/A = 3.6, S/A = 4, and curing of 28 and 90 days are considered. We can identify that the water absorption reduces with the increase in days. It depends on the mix proportions and ratios used in the mix, and it also depends on the size of the particles. If there is any reduction in the S/A ratio, a decrease in absorption is identified in concrete

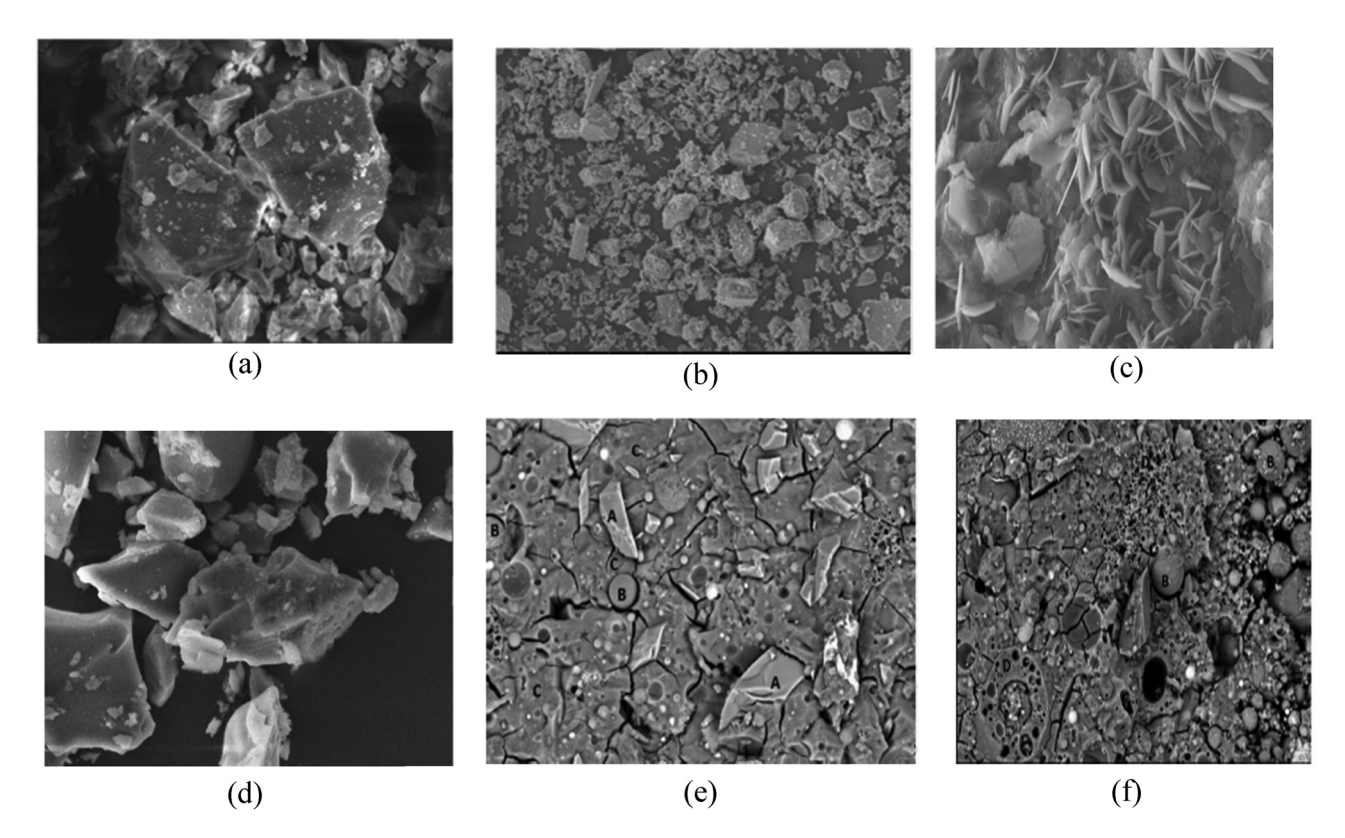


Figure 8: SEM images for hardened concrete: (a-c) [104]; (d) [105]; (e and f) [24].

Figure 9: Water absorption for different mix proportions.

DE GRUYTER

with high MK content. The water absorption also depends on additives added to the mix [148]. The fourth bar in Figure 9 shows water absorption for Na₂O (%) content for 7 and 28 days. We can observe that the water absorption decreases with an increase in days. This is because as time passes, concrete becomes dense, and porosity is less, so there is no scope for water adsorption, so water adsorption decreases with an increase in days. Cementitious mortars absorbed more water at 7 and 28 days than activated alkali mortars [121]. The fifth set of bars in Figure 9 shows water absorption for different proportions of FAGPC with TiO₂. Here, we can observe less water absorption by introducing nano-TiO₂ content. In this plot, FA-NT 0, FA-NT 1, FA-NT 2, FA-NT 3, FA-NT 4, and FA-NT 5 means 0, 1, 2, 3, 4, and 5% of nano-TiO2. This plot shows that no nano-TiO2 water absorption is more. This is because nano-TiO2 contains finer particles, and water absorption is more [131].

The sixth set of bars in Figure 9 shows water absorption for different mix proportions for mortar for AAFA-0.6, AAFA-0.7, AAFA-0.8, AAFAS8/2, AAFAS6/4, and SPC is considered in this plot. It can be observed that the dried pastes realize more water as the liquid/ratio or slag replacement increases. The water-filled space can be regarded as porosity, between 37.0 and 42.2% in the cement pastes. The water absorption for the mortars is much more stable than the binders. It can be attributed that all porosities of the AAFA mortars are very close together [149]. In summary, durability properties mainly focus on the resistance of concrete or mortar to different temperatures and

pressures. The water absorption for the mortars is much more constant than the binders.

5 Conclusions

An extensive review of the impact of SPs on geopolymer mortar and concrete is analyzed, and the following conclusions were made:

- The addition of SPs like PCE is more effective than other SPs and gives the required workability. SPs should be added to the required quantity. If more of it is added, it leads to undesired workability. Chemical admixtures afford enhanced workability, allowing for better geopolymer binder and aggregates' dispersion and improving strength due to better interfacial bonding. So should be very specific in the selection of Chemical admixtures. When selecting SPs, it is important to consider their environmental impact and compatibility with the sustainable goals of geopolymer technology.
- The setting rate depends on the type of additives, and it will be accelerated with increased calcium content. When slag content is increased in the mix, the initial setting time is reduced due to more alumina in the slag. The setting of geopolymer concrete or mortar happens when SiO_2 and $\mathrm{Al}_2\mathrm{O}_3$ particles react with an alkaline solution more than the $\mathrm{Al}_2\mathrm{O}_3$ particles' rapid setting occurs.

- Consistency of concrete increases as supplementary components are added. This is because of the fineness of supplementary components which are added.
- If fine particles are more in the mix, the workability will be greater because it takes more time to set. The presence of fine particles also leads to better particle distribution. This is because the finer the particles more surface area increases, so it takes more time to complete the reaction process.
- SMF (sulfonated melamine formaldehyde) SPs have lower compressive strength than others because SMF has alkali medium instability, giving less compressive strength. This is because the sulfonate groups may affect the cross-linking density and interactions between the polymer chains which leads to the reduction of compressive strength. The sulfonate groups undergo hydrolysis reactions. Sulfonate groups are susceptible to hydrolysis in alkaline conditions, which leads to a reduction in their effectiveness and stability.
- Flexural strength increases with an increase in sodium hydroxide concentration. High calcium content helps increase the flexural content up to a certain limit. With the introduction of an SP, the strength increases slowly.
- SEM images show the structure of particles that we use in mixing. These images are very important because, by the images, we can know about the particular structure and its voids.
- Field trials and thorough testing should be conducted to determine the optimal type and dosage of SP for specific geopolymer formulations and application conditions.
- Water absorption mainly depends on the pores and size of the particles in the concrete or mortar. Water absorption decreases with the increase in silica content.

At the outset, the usage of SPs improves the geopolymer properties upon their desired dosages; more dosage leads to reduced performance.

Acknowledgments: The authors would like to acknowledge the support of Prince Sultan University for paying the Article Processing Charges (APC) of this publication.

Funding information: Prince Sultan University funded the Article Processing Charges (APC) of this publication.

Author contributions: All authors have accepted responsibility for the entire content of this manuscript and approved its submission.

Conflict of interest: The authors state no conflict of interest.

References

- [1] Tosti, L., A. van Zomeren, J. R. Pels, and R. N. J. Comans. Technical and environmental performance of lower carbon footprint cement mortars containing biomass fly ash as a secondary cementitious material. *Resources, Conservation and Recycling*, Vol. 134, No. January, 2018, pp. 25–33.
- [2] Palacios, M., P. F. G. Banfill, and F. Puertas. Rheology and setting of alkali-activated slag pastes and mortars: Effect if organic admixture. ACI Materials Journal, Vol. 105, No. 2, 2008, pp. 140–148.
- [3] Tong, S., Z. Yuqi, and W. Qiang. Recent advances in chemical admixtures for improving the workability of alkali-activated slagbased material systems. *Construction and Building Materials*, Vol. 272, 2021, id. 121647.
- [4] Gunasekara, C., D. W. Law, S. Setunge, and J. G. Sanjayan. Zeta potential, gel formation and compressive strength of low calcium fly ash geopolymers. *Construction and Building Materials*, Vol. 95, 2015, pp. 592–599.
- [5] Kong, Y. K. and K. Kurumisawa. Prediction of the drying shrinkage of alkali-activated materials using artificial neural networks. Case Studies in Construction Materials, Vol. 17, No. April, 2022, id. e01166.
- [6] Costa, F. N. and D. V. Ribeiro. Reduction in CO2 emissions during production of cement, with partial replacement of traditional raw materials by civil construction waste (CCW). *Journal of Cleaner Production*, Vol. 276, 2020, id. 123302.
- [7] Yunsheng, Z., S. Wei, L. Zongjin, Z. Xiangming, C. Eddie, and C. Chungkong. Impact properties of geopolymer based extrudates incorporated with fly ash and PVA short fiber. *Construction and Building Materials*, Vol. 22, No. 3, 2008, pp. 370–383.
- [8] Naik, T. R. Sustainability of concrete construction. *Practice Periodical on Structural Design and Construction*, Vol. 13, No. 2, 2008, pp. 98–103.
- [9] Shi, C., C. Meyer, and A. Behnood. Utilization of copper slag in cement and concrete. *Resources, Conservation and Recycling*, Vol. 52, No. 10, 2008, pp. 1115–1120.
- [10] Chand, G. Microstructural study of sustainable cements produced from industrial by-products, natural minerals and agricultural wastes: A critical review on engineering properties. Cleaner Engineering and Technology, Vol. 4, No. July, 2021, id. 100224.
- [11] Garcia Lodeiro, I., N. Cristelo, A. Palomo, and A. Fernández-Jiménez. Use of industrial by-products as alkaline cement activators. Construction and Building Materials, Vol. 253, 2020, id. 119000.
- [12] Mavroulidou, M., I. Sanam, and L. Mengasini. Mechanical and durability performance of alkali-activated slag cement concretes with carbonate and silicate activators. Sustainable Chemistry and Pharmacy, Vol. 31, 2023, id. 100896.
- [13] Murali, G. Recent research in mechanical properties of geopolymer-based ultra-high-performance concrete: A review. *Defence Technology*, July, 2023.
- [14] Zaid, O., N. Abdulwahid Hamah Sor, R. Martínez-García, J. de Prado-Gil, K. Mohamed Elhadi, and A. M. Yosri. Sustainability evaluation, engineering properties and challenges relevant to geopolymer concrete modified with different nanomaterials: A systematic review. Ain Shams Engineering Journal, Vol. 15, No. 2, 2023, id. 102373.
- [15] Kishore, K., A. Pandey, N. K. Wagri, A. Saxena, J. Patel, and A. Al-Fakih. Technological challenges in nanoparticle-modified geopolymer concrete: A comprehensive review on nanomaterial dispersion, characterization techniques and its mechanical

- properties. Case Studies in Construction Materials, Vol. 19, No. July, 2023. id. e02265.
- [16] Duxson, P., J. L. Provis, G. C. Lukey, and J. S. J. van Deventer. The role of inorganic polymer technology in the development of 'green concrete'. Cement and Concrete Research, Vol. 37, No. 12, 2007, pp. 1590-1597.
- Kanagaraj, B., N. Anand, S. Raj R, and E. Lubloy. Performance [17] evaluation of sodium silicate waste as a replacement for conventional sand in geopolymer concrete. Journal of Cleaner Production, Vol. 375, No. September, 2022, id. 134172.
- Wasim, M., T. Duc Ngo, and D. Law. Durability performance of reinforced waste-based geopolymer foam concrete under exposure to various corrosive environments. Case Studies in Construction Materials, Vol. 15, No. August, 2021, id. e00703.
- [19] Milad, A., Ali A. S. B., Babalghaith A. M. Memon Z. A. Mashaan N. S. Arafa, et al. Utilisation of waste-based geopolymer in asphalt pavement modification and construction—A review. Sustainability, Vol. 13, No. 6, 2021, id. 3330.
- Alharbi, Y. R., A. A. Abadel, A. A. Salah, O. A. Mayhoub, and M. Kohail. Engineering properties of alkali activated materials reactive powder concrete. Construction and Building Materials, Vol. 271, 2021, id. 121550.
- [21] Dehghani, A., F. Aslani, and N. Ghaebi Panah. Effects of initial SiO2/Al2O3 molar ratio and slag on fly ash-based ambient cured geopolymer properties. Construction and Building Materials, Vol. 293, 2021, id. 123527.
- [22] Bajgain, S. K. and M. Mookherjee. Carbon bearing aluminosilicate melt at high pressure. Geochimica et Cosmochimica Acta, Vol. 312, 2021, pp. 106-123.
- [23] Le Losq, C., A. P. Valentine, B. O. Mysen, and D. R. Neuville. Structure and properties of alkali aluminosilicate glasses and melts: Insights from deep learning. Geochimica et Cosmochimica Acta, Vol. 314, 2021, pp. 27-54.
- [24] Nath, P. and P. K. Sarker. Effect of GGBFS on setting, workability and early strength properties of fly ash geopolymer concrete cured in ambient condition. Construction and Building Materials, Vol. 66, Sep. 2014, pp. 163-171.
- Abdullah M. N. I., F. Mustapha, K. A. Ahmad, M. Mustapha, T. [25] Khan, B. Singh, et al. Effect of different pre-treatment on the microstructure and intumescent properties of rice husk ashbased geopolymer hybrid coating. Polymers (Basel), Vol. 14, No. 11, 2022, id. 2252.
- [26] Liu, J., J. H. Doh, D. E. L. Ong, Z. Liu, and M. N. S. Hadi. Methods to evaluate and quantify the geopolymerization reactivity of wastederived aluminosilicate precursor in alkali-activated material: A state-of-the-art review. Construction and Building Materials, Vol. 362, No. August 2022, 2023, id. 129784.
- [27] Gharzouni, A., L. Ouamara, I. Sobrados, and S. Rossignol. Alkaliactivated materials from different aluminosilicate sources: Effect of aluminum and calcium availability. Journal of Non-Crystalline Solids, Vol. 484, No. January, 2018, pp. 14-25.
- [28] Ouffa, N., M. Benzaazoua, T. Belem, R. Trauchessec, and A. Lecomte. Alkaline dissolution potential of aluminosilicate minerals for the geosynthesis of mine paste backfill. Materials Today Communications, Vol. 24, No. September, 2020, id. 2019.
- [29] Nath, P., P. K. Sarker, and V. B. Rangan. Early age properties of low-calcium fly ash geopolymer concrete suitable for ambient curing. Procedia Engineering, Vol. 125, 2015, pp. 601-607.
- Laskar, S. M. and S. Talukdar. Preparation and tests for workability, compressive and bond strength of ultra-fine slag based

- geopolymer as concrete repairing agent. Construction and Building Materials, Vol. 154, Nov. 2017, pp. 176-190.
- [31] Chindaprasirt, P., T. Chareerat, and V. Sirivivatnanon. Workability and strength of coarse high calcium fly ash geopolymer. Cement and Concrete Composites, Vol. 29, No. 3, 2007, pp. 224-229.
- Ravitheja, A. and N. L. N. Kiran Kumar. A study on the effect of nano clay and GGBS on the strength properties of fly ash based geopolymers. Materials Today: Proceedings, Vol. 19, 2019, pp. 273-276.
- [33] Paul, E. Influence of superplasticizer on workability and strength of ambient cured alkali activated mortar. Cleaner Materials, Vol. 6, Dec. 2022, id. 100152.
- [34] Krishna Rao, A. and D. Rupesh Kumar. Effect of various alkaline binder ratio on geopolymer concrete under ambient curing condition. Materials Today: Proceedings, Vol. 27, 2020, pp. 1768-1773.
- [35] Ihsan, A. Use of waste glass powder toward more sustainable geopolymer concrete. Journal of materials research and technology, Vol. 24, 2023, pp. 8533-8546.
- [36] Siyal, A. A., M. R. Shamsuddin, S. H. Khahro, A. Low, and M. Ayoub. Optimization of synthesis of geopolymer adsorbent for the effective removal of anionic surfactant from aqueous solution. Journal of Environmental Chemical Engineering, Vol. 9, No. 1, 2021, id. 104949.
- [37] Nematollahi, B. and J. Sanjayan. Effect of different superplasticizers and activator combinations on workability and strength of fly ash based geopolymer. Materials & Design, Vol. 57, 2014, pp. 667-672.
- [38] Richardson, I. G. Tobermorite/jennite- and tobermorite/calcium hydroxide-based models for the structure of C-S-H: Applicability to hardened pastes of tricalcium silicate, β-dicalcium silicate, Portland cement, and blends of Portland cement with blast-furnace slag, metakaol. Cement and Concrete Research, Vol. 34, No. 9, 2004, pp. 1733-1777.
- [39] Mabroum, S., S. Moukannaa, A. El Machi, Y. Taha, M. Benzaazoua, and R. Hakkou. Mine wastes based geopolymers: A critical review. Cleaner Engineering and Technology, Vol. 1, 2020, id. 100014.
- Sandeep Kumar, A. D., D. Singh, V. S. Reddy, and K. J. Reddy. Geopolymerization mechanism and factors affecting it in Metakaolinslag-fly ash blended concrete. E3S Web Conference, Vol. 184, 2020, pp. 1-6.
- Jamaludin L., R. A. Razak, M. M. A. B. Abdullah, P. Vizureanu, A. [41] Bras, T. Imjai, et al. The suitability of photocatalyst precursor materials in geopolymer coating applications: A review. Coatings, Vol. 12, No. 9, 2022, id. 1348.
- [42] Shilar, F. A., S. V. Ganachari, V. B. Patil, N. Almakayeel, and T. M. Yunus Khan. Development and optimization of an eco-friendly geopolymer brick production process for sustainable masonry construction. Case Studies in Construction Materials, Vol. 18, No. March, 2023, id. e02133.
- Shilar, F. A., S. V. Ganachari, V. B. Patil, I. Neelakanta Reddy, and J. [43] Shim. Preparation and validation of sustainable metakaolin based geopolymer concrete for structural application. Construction and Building Materials, Vol. 371, No. February, 2023, id. 130688.
- Shilar, F. A., S. V. Ganachari, V. B. Patil, S. Javed, T. M. Y. Khan, and [44] R. U. Baig. Assessment of destructive and nondestructive analysis for GGBS based geopolymer concrete and its statistical analysis. Polymers (Basel), Vol. 14, No. 15, 2022.
- [45] Shilar, F. A., S. V. Ganachari, V. B. Patil, T. M. Y. Khan, S. Javed, and R. U. Baig. Optimization of alkaline activator on the strength

- properties of geopolymer concrete. *Polymers (Basel)*, Vol. 14, No. 12, 2022.
- [46] Shilar, F. A., S. V. Ganachari, V. B. Patil, K. S. Nisar, A. H. Abdel-Aty, and I. S. Yahia. Evaluation of the effect of granite waste powder by varying the molarity of activator on the mechanical properties of ground granulated blast-furnace slag-based geopolymer concrete. *Polymers (Basel)*, Vol. 14, No. 2, 2022, id. 306.
- [47] Marvila, M. T., A. R. Garcez de Azevedo, J. A. Tostes Linhares Júnior, and C. M. Fontes Vieira. Activated alkali cement based on blast furnace slag: effect of curing type and concentration of Na20. *Journal of Materials Research and Technology*, Vol. 23, 2023, pp. 4551–4565.
- [48] Shee-Ween, O., H. Cheng-Yong, L. Yun-Ming, M. M. A. B. Abdullah, H. Li-Ngee, P. Pakawanit, et al. Green development of fly ash geopolymer via casting and pressing approaches: Strength, morphology, efflorescence and ecological properties. *Construction and Building Materials*, Vol. 398, No. November 2022, 2023, id. 132446.
- [49] Shilar, F. A., S. V. Ganachari, V. B. Patil, B. E. Bhojaraja, T. M. Yunus Khan, and N. Almakayeel. A review of 3D printing of geopolymer composites for structural and functional applications. *Construction and Building Materials*, Vol. 400, No. February, 2023, id. 132869.
- [50] Wan-En, O., L. Yun-Ming, H. Cheng-Yong, M. M. A. B. Abdullah, H. L. Ngee, P. Pakawanit, et al. Acid-resistance of one-part geopolymers: Sodium aluminate and carbonate as alternative activators to conventional sodium metasilicate and hydroxide. *Construction and Building Materials*, Vol. 404, No. September, 2023, id. 133264.
- [51] Shilar, F. A., S. V. Ganachari, and V. B. Patil. Investigation of the effect of granite waste powder as a binder for different molarity of geopolymer concrete on fresh and mechanical properties. *Materials Letters*, Vol. 309, No. October 2021, 2022, id. 131302.
- [52] Al-Noaimat, Y. A., S. H. Ghaffar, M. Chougan, and M. J. Al-Kheetan. A review of 3D printing low-carbon concrete with one-part geo-polymer: Engineering, environmental and economic feasibility. Case Studies in Construction Materials, Vol. 18, No. October 2022, 2023. id. e01818.
- [53] Islam, A., U. J. Alengaram, M. Z. Jumaat, I. I. Bashar, and S. M. A. Kabir. Engineering properties and carbon footprint of ground granulated blast-furnace slag-palm oil fuel ash-based structural geopolymer concrete. *Construction and Building Materials*, Vol. 101, 2015, pp. 503–521.
- [54] Garces, J. I. T., A. B. Beltran, R. R. Tan, J. M. C. Ongpeng, and M. A. B. Promentilla. Carbon footprint of self-healing geopolymer concrete with variable mix model. *Cleaner Chemical Engineering*, Vol. 2, No. May, 2022, id. 100027.
- [55] Jegan, M., R. Annadurai, and P. R. Kannan Rajkumar. A state of the art on effect of alkali activator, precursor, and fibers on properties of geopolymer composites. *Case Studies in Construction Materials*, Vol. 18, No. January, 2023, id. e01891.
- [56] Neupane, K. Evaluation of environmental sustainability of onepart geopolymer binder concrete. *Cleaner Materials*, Vol. 6, No. 2, 2022, id. 100138.
- [57] Saini, G. and U. Vattipalli. Assessing properties of alkali activated GGBS based self-compacting geopolymer concrete using nanosilica. Case Studies in Construction Materials, Vol. 12, 2020, id. e00352.
- [58] Xie, J. and O. Kayali. Effect of SP on workability enhancement of Class F and Class C fly ash-based geopolymers. Construction and Building Materials, Vol. 122, 2016, pp. 36–42.
- [59] Pandurangan, K., M. Thennavan, and A. Muthadhi. Studies on effect of source of flyash on the bond strength of geopolymer

- concrete. *Materials Today: Proceedings*, Vol. 5, No. 5, 2018, pp. 12725–12733.
- [60] de Hita, M. J. and M. Criado. Influence of superplasticizers on the workability and mechanical development of binary and ternary blended cement and alkali-activated cement. *Construction and Building Materials*, Vol. 366, No. January, 2023, id. 130272.
- [61] Bakharev, T., J. G. Sanjayan, and Y. B. Cheng. Effect of admixtures on properties of alkali-activated slag concrete. *Cement and Concrete Research*, Vol. 30, No. 9, 2000, pp. 1367–1374.
- [62] Lloyd, N. A. and B. V. Rangan. Geopolymer concrete with fly ash. 2nd International Conference on sustainable construction Materials and Technologies, Vol. 7, 2010, pp. 1493–1504.
- [63] Kandagaddala, R. K., S. V. Dhanapal, and P. Nanthagopalan. Rheological characterization of limestone calcined clay cement pastes with various generations of superplasticizers for pumping applications. *Journal of Building Engineering*, Vol. 76, No. March, 2023, id. 107410.
- [64] Sha, S., S. Mantellato, S. A. Weckwerth, Z. Zhang, C. Shi, and R. J. Flatt. Do superplasticizers work the way we think? New insights from their effect on the percolation threshold of limestone pastes. *Cement and Concrete Research*, Vol. 172, No. July, 2023, id. 107235.
- [65] Vora, P. R. and U. V. Dave. Parametric studies on compressive strength of geopolymer concrete. *Procedia Engineering*, Vol. 51, 2013, pp. 210–219.
- [66] Sherwani, A. F. H., K. H. Younis, R. W. Arndt, and K. Pilakoutas. Performance of self-compacted geopolymer concrete containing fly ash and slag as binders. Sustainability, Vol. 14, No. 22, Nov. 2022.
- [67] Rajendrana, R., D. S. Kumar, K. Megan, P. Muneswaren, D. Senthilvel, B. Shri, et al. Strength analysis of geopolymer concrete based on fly ash and P-sand. *Materials Today: Proceedings*, Vol. 47, 2021, pp. 5489–5492.
- [68] Almutairi, A. L., B. A. Tayeh, A. Adesina, H. F. Isleem, and A. M. Zeyad. Potential applications of geopolymer concrete in construction: A review. *Case Studies in Construction Materials*, Vol. 15, No. August, 2021, id. e00733.
- [69] Mahmood, A. H., S. J. Foster, and A. Castel. Effects of mixing duration on engineering properties of geopolymer concrete. *Construction and Building Materials*, Vol. 303, No. April, 2021, id. 124449.
- [70] Negahban, E., A. Bagheri, and J. Sanjayan. Pore structure profile of ambient temperature-cured geopolymer concrete and its effect on engineering properties. *Construction and Building Materials*, Vol. 406, No. April, 2023, id. 133311.
- [71] Kugler, F., J. Karrer, W. Krcmar, and U. Teipel. Setting behavior and mechanical properties of concrete rubble fly ash geopolymers. *Open Ceramics*, Vol. 11, May, 2022, id. 100286.
- [72] Asadi, I., M. H. Baghban, M. Hashemi, N. Izadyar, and B. Sajadi. Phase change materials incorporated into geopolymer concrete for enhancing energy efficiency and sustainability of buildings: A review. Case Studies in Construction Materials, Vol. 17, No. March, 2022, id. e01162.
- [73] Amran, M., A. Al-Fakih, S. H. Chu, R. Fediuk, S. Haruna, A. Azevedo, et al. Long-term durability properties of geopolymer concrete: An in-depth review. *Case Studies in Construction Materials*, Vol. 15, No. August, 2021, id. e00661.
- [74] Çelik, A.İ., Y. O. Özkılıç, A. Bahrami, and I. Y. Hakeem. Mechanical performance of geopolymer concrete with micro silica fume and waste steel lathe scraps. *Case Studies in Construction Materials*, Vol. 19, October, 2023, id. e02548.

- [75] Martínez, A. and S. A. Miller. A review of drivers for implementing geopolymers in construction: Codes and constructability. Resources, Conservation and Recycling, Vol. 199, October, 2023, id. 107238.
- [76] Mayhoub, O. A., E. S. A. R. Nasr, Y. Ali, and M. Kohail. Properties of slag based geopolymer reactive powder concrete. Ain Shams Engineering Journal, Vol. 12, No. 1, 2021, pp. 99-105.
- [77] Chandra, S. and I. Biörnström. Influence of cement and superplasticizers type and dosage on the fluidity of cement mortars -Part I. Cement and Concrete Research, Vol. 32, No. 10, 2002, pp. 1605-1611.
- [78] Kapeluszna, E. and K. Chrabaszcz. Mutual compatibility of superplasticizers (PC, SNF), grinding aids (TEA, glycol) and C3A in Portland cement systems - Hydration, rheology, physical properties and air void characteristics. Construction and Building Materials, Vol. 373, January, 2023, id. 130877.
- [79] De Schutter, G., M. Ezzat, K. Lesage, and R. Hoogenboom. Responsive superplasticizers for active rheology control of cementitious materials. Cement and Concrete Research, Vol. 165, No. January, 2023, id. 107084.
- [88] Gupta, N., A. Gupta, K. K. Saxena, A. Shukla, and S. K. Goyal. Mechanical and durability properties of geopolymer concrete composite at varying superplasticizer dosage. Materials Today: Proceedings, Vol. 44, 2021, pp. 12-16.
- [81] Triwulan, M., P. Wigestika, and J. J. Ekaputri. Addition of superplasticizer on geopolymer concrete. ARPN Journal of Engineering and Applied Sciences, Vol. 11, No. 24, 2016, pp. 14456-14462.
- [82] Palacios, M., Y. F. Houst, P. Bowen, and F. Puertas. Adsorption of superplasticizer admixtures on alkali-activated slag pastes. Cement and Concrete Research, Vol. 39, No. 8, 2009, pp. 670-677.
- [83] Palacios, M. and F. Puertas. Effect of superplasticizer and shrinkage-reducing admixtures on alkali-activated slag pastes and mortars. Cement and Concrete Research, Vol. 35, No. 7, 2005, pp. 1358-1367.
- [84] Sathonsaowaphak, A., P. Chindaprasirt, and K. Pimraksa. Workability and strength of lignite bottom ash geopolymer mortar. Journal of Hazardous Materials, Vol. 168, No. 1, 2009,
- [85] lang, J. G., N. K. Lee, and H. K. Lee. Fresh and hardened properties of alkali-activated fly ash/slag pastes with superplasticizers. Construction and Building Materials, Vol. 50, 2014, pp. 169-176.
- Bong, S. H., B. Nematollahi, A. Nazari, M. Xia, and J. Sanjayan. [86] Efficiency of different superplasticizers and retarders on properties of 'one-part' fly ash-slag blended geopolymers with different activators. Materials (Basel), Vol. 12, No. 20, 2019, id. 3410.
- [87] Yin, W., X. Li, Y. Chen, Y. Wang, M. Xu, and C. Pei. Mechanical and rheological properties of High-Performance concrete (HPC) incorporating waste glass as cementitious material and fine aggregate. Construction and Building Materials, Vol. 387, No. December 2022, 2023, id. 131656.
- [88] Rifaai, Y., A. Yahia, S. Aggoun, and E. H. Kadri. Rheology and mechanical performance of self-consolidating hybrid-geopolymer concrete as a sustainable construction material. Construction and Building Materials, Vol. 314, No. PB, 2022, id. 125633.
- [89] Wang, W., C. Fan, B. Wang, X. Zhang, and Z. Liu. Workability, rheology, and geopolymerization of fly ash geopolymer: Role of alkali content, modulus, and waterbinder ratio. Construction and Building Materials, Vol. 367, No. November 2022, 2023, id. 130357.
- Gadkar, A. and K. V. L. Subramaniam. Porosity and pore structure control in cellular geopolymer using rheology and surface

- tension modifiers. Construction and Building Materials, Vol. 323, No. December 2021, 2022, id. 126600.
- [91] Zhang, D. W., K. F. Zhao, F. Zhu Xie, H. Li, and D. Min Wang. Rheology and agglomerate structure of fresh geopolymer pastes with different Ms ratio of waterglass. Construction and Building Materials, Vol. 250, 2020, id. 118881.
- [92] Zhang, D. W., K. F. Zhao, F. Zhu Xie, H. Li, and D. Min Wang. Effect of water-binding ability of amorphous gel on the rheology of geopolymer fresh pastes with the different NaOH content at the early age. Construction and Building Materials, Vol. 261, 2020, id. 120529.
- [93] Panda, B., C. Unluer, and M. J. Tan. Extrusion and rheology characterization of geopolymer nanocomposites used in 3D printing. Composites Part B: Engineering, Vol. 176, No. August, 2019, id 107290
- [94] Revathi, T. and R. Jeyalakshmi. Fly ash-GGBS geopolymer in boron environment: A study on rheology and microstructure by ATR FT-IR and MAS NMR. Construction and Building Materials, Vol. 267, 2021, id. 120965.
- [95] Hadi, M. N. S., H. Zhang, and S. Parkinson. Optimum mix design of geopolymer pastes and concretes cured in ambient condition based on compressive strength, setting time and workability. Journal of Building Engineering, Vol. 23, No. February, 2019, pp. 301-313.
- [96] Neville, J. J. B. A. M. Concrete technology by A. M. Neville and J.J-By EasyEngineering.net, Vol. 2, 2010, pp. 1-434.
- [97] Wu, X., Y. Shen, and L. Hu. Performance of geopolymer concrete activated by sodium silicate and silica fume activator. Case Studies in Construction Materials, Vol. 17, No. August, 2022, id. e01513.
- [98] Shen, P., P. Han, T. Guo, R. Wang, W. Song, X. Bai, et al. Study on the Setting and Hardening Process of red mud-coal metakaolin geopolymer concrete by Electrochemical Impedance Spectroscopy. International Journal of Electrochemical Science, Vol. 17, No. 11, 2022, id. 221158.
- [99] Arunkumar, K., M. Muthukannan, A. Suresh kumar, and A. Chithambar Ganesh. Mitigation of waste rubber tire and waste wood ash by the production of rubberized low calcium waste wood ash based geopolymer concrete and influence of waste rubber fibre in setting properties and mechanical behavior. Environmental Research, Vol. 194, No. October 2020, 2021, id. 110661.
- [100] Tran, M. V., T. H. Vu, and T. H. Y. Nguyen. Simplified assessment for one-part 3D-printable geopolymer concrete based on slump and slump flow measurements. Case Studies in Construction Materials, Vol. 18, No. September 2022, 2023, id. e01889.
- Abdellatief, M., M. Mortagi, M. A. Elrahman, A. M. Tahwia, A. E. Allugmani, and H. Alanazi. Characterization and optimization of fresh and hardened properties of ultra-high performance geopolymer concrete. Case Studies in Construction Materials, Vol. 19, No. April, 2023, id. e02549.
- [102] Jaji, M. B., G. P. A. G. van Zijl, and A. J. Babafemi. Slag-modified metakaolin-based geopolymer for 3D concrete printing application: Evaluating fresh and hardened properties. Cleaner Engineering and Technology, Vol. 15, No. May, 2023, id. 100665.
- [103] Tayeh, B. A., M. H. Akeed, S. Qaidi, and B. H. A. Bakar. Influence of microsilica and polypropylene fibers on the fresh and mechanical properties of ultra-high performance geopolymer concrete (UHP-GPC). Case Studies in Construction Materials, Vol. 17, No. July, 2022, id. e01367.
- Γ1041 Bian, Z., G. Jin, and T. Ji. Effect of combined activator of Ca(OH)2 and Na2CO3 on workability and compressive strength of alkali-

- activated ferronickel slag system. *Cement and concrete composites*, Vol. 123, No. June, 2021, id. 104179.
- [105] Zhao, J., B. Long, G. Yang, Z. Cheng, and Q. Liu. Characteristics of alkali-activated slag powder mixing with seawater: Workability, hydration reaction kinetics and mechanism. *Case Studies in Construction Materials*, Vol. 17, No. August, 2022, id. e01381.
- [106] Mohapatra, A. K. and B. Pradhan. Hybrid alkali activated cements (HAACs) system: A state-of-the-art review on fresh, mechanical, and durability behaviour. *Construction and Building Materials*, Vol. 361, No. October, 2022, id. 129636.
- [107] Lee, T. and J. Lee. Setting time and compressive strength prediction model of concrete by nondestructive ultrasonic pulse velocity testing at early age. *Construction and Building Materials*, Vol. 252, 2020, id. 119027.
- [108] Babu, G. K., K. V. Rao, S. Dey, and G. T. N. Veerendra. Performance studies on quaternary blended geopolymer concrete. *Hybrid Advances*, Vol. 2, No. December 2022, 2023, id. 100019.
- [109] Nayak, D. K., P. P. Abhilash, R. Singh, R. Kumar, and V. Kumar. Fly ash for sustainable construction: A review of fly ash concrete and its beneficial use case studies. *Cleaner Materials*, Vol. 6, No. June, 2022, id. 100143.
- [110] Collins, F. G. and J. G. Sanjayan. Workability and mechanical properties of alkali activated slag concrete. *Cement and Concrete Research*, Vol. 29, No. 3, 1999, pp. 455–458.
- [111] Fang, G., W. K. Ho, W. Tu, and M. Zhang. Workability and mechanical properties of alkali-activated fly ash-slag concrete cured at ambient temperature. *Construction and Building Materials*, Vol. 172, 2018, pp. 476–487.
- [112] Nurruddin, M. F., H. Sani, B. S. Mohammed, and I. Shaaban. Methods of curing geopolymer concrete: A review. *International Journal of Advanced and Applied Sciences*, Vol. 5, No. 1, 2018, pp. 31–36
- [113] Padmakar, M., B. Barhmaiah, and M. L. Priyanka. Characteristic compressive strength of a geo polymer concrete. *Materials Today: Proceedings*, Vol. 37, No. Part 2, 2020, pp. 2219–2222.
- [114] Mohe, N. S., Y. W. Shewalul, and E. C. Agon. Experimental investigation on mechanical properties of concrete using different sources of water for mixing and curing concrete. *Case Studies in Construction Materials*, Vol. 16, No. February, 2022, id. e00959.
- [115] Ge, X., Y. Liu, Y. Mao, X. Hu, and C. Shi. Characteristics of fly ash-based geopolymer concrete in the field for 4 years. *Construction and Building Materials*, Vol. 382, No. April, 2023, id. 131222.
- [116] Shashikant G., and G. Prince Arulraj. A research article on 'Geopolymer concrete'. *International Journal of Innovative Technology and Exploring Engineering*, Vol. 8, No. 9 Special Issue 2, Jul. 2019, pp. 499–502.
- [117] Qian, L. P., B. T. Huang, L. Y. Xu, and J. G. Dai. Concrete made with high-strength artificial geopolymer aggregates: Mechanical properties and failure mechanisms. *Construction and Building Materials*, Vol. 367, No. September 2022, 2023, id. 130318.
- [118] Sun, Y., Z. Liu, S. Ghorbani, G. Ye, and G. De Schutter. Fresh and hardened properties of alkali-activated slag concrete: The effect of fly ash as a supplementary precursor. *Journal of Cleaner Production*, Vol. 370, No. August, 2022, id. 133362.
- [119] Rakngan, W., T. Williamson, R. D. Ferron, G. Sant, and M. C. G. Juenger. Controlling workability in alkali-activated Class C fly ash. Construction and Building Materials, Vol. 183, 2018, pp. 226–233.
- [120] Oderji, S. Y., B. Chen, C. Shakya, M. R. Ahmad, and S. F. A. Shah. Influence of superplasticizers and retarders on the workability and strength of one-part alkali-activated fly ash/slag binders

- cured at room temperature. *Construction and Building Materials*, Vol. 229, 2019, id. 116891.
- [121] Marvila, M. T., A. R. G. de Azevedo, L. B. de Oliveira, G. de Castro Xavier, and C. M. F. Vieira. Mechanical, physical and durability properties of activated alkali cement based on blast furnace slag as a function of %Na2O. *Case Studies in Construction Materials*, Vol. 15, No. September, 2021, id. e00723.
- [122] Tashan, J. Flexural behavior evaluation of repaired high strength geopolymer concrete. *Composite Structures*, Vol. 300, No. June, 2022, id. 116144.
- [123] Moon, D. Y. Flexural behavior of concrete beams reinforced with high-strength steel bars. *Journal of the Korean Society of Hazard Mitigation*, Vol. 13, No. 6, 2013, pp. 107–113.
- [124] Tournier M., P. Goulet, N. Fonvieille, D. Nerini, and M. Johnson. Journal of Marine Systems, 2020, id. 103608.
- [125] Ahmed, H. Q., D. K. Jaf, and S. A. Yaseen. Flexural strength and failure of geopolymer concrete beams reinforced with carbon fibre-reinforced polymer bars. *Construction and Building Materials*, Vol. 231, 2020, id. 117185.
- [126] Lin Chan, C. and M. Zhang. Effect of limestone on engineering properties of alkali-activated concrete: A review. Construction and Building Materials, Vol. 362, Jan. 2023, id. 29709.
- [127] Zerfu, K. and J. J. Ekaputri. The effect of reinforcement ratio on the flexural performance of alkali-activated fly ash-based geopolymer concrete beam. *Heliyon*, Vol. 8, No. 12, 2022, id. e12015.
- [128] Zhong, H. and M. Zhang. Dynamic splitting tensile behaviour of engineered geopolymer composites with hybrid polyvinyl alcohol and recycled tyre polymer fibres. *Journal of Cleaner Production*, Vol. 379, Dec. 2022, id. 134779.
- [129] Pacheco-Torgal, F., D. Moura, Y. Ding, and S. Jalali. Composition, strength and workability of alkali-activated metakaolin based mortars. *Construction and Building Materials*, Vol. 25, No. 9, 2011, pp. 3732–3745.
- [130] Xu, J., A. Kang, Z. Wu, P. Xiao, and Y. Gong. Effect of high-calcium basalt fiber on the workability, mechanical properties and microstructure of slag-fly ash geopolymer grouting material. *Construction and Building Materials*, Vol. 302, No. March, 2021, id. 124089.
- [131] Sastry, K. V. S. G. K., P. Sahitya, and A. Ravitheja. Influence of nano TiO₂ on strength and durability properties of geopolymer concrete. *Materials Today: Proceedings*, Vol. 45, 2021, pp. 1017–1025.
- [132] Jithendra, C. and S. Elavenil. Role of superplasticizer on GGBS based geopolymer concrete under ambient curing. *Materials Today: Proceedings*, Vol. 18, 2019, pp. 148–154.
- [133] Chen, C., X. Zhang, and H. Hao. Dynamic tensile properties of geopolymer concrete and fibre reinforced geopolymer concrete. *Construction and Building Materials*, Vol. 393, No. June, 2023, id. 132159.
- [134] Umesh B. Mechanical and durability properties of standard and high strength geopolymer concrete using particle packing theory. *Construction and Building Materials*, Vol. 400, No. August, 2023, id. 132722.
- [135] Tahwia, A. M., M. A. Ellatief, G. Bassioni, A. M. Heniegal, and M. A. Elrahman. Influence of high temperature exposure on compressive strength and microstructure of ultra-high performance geopolymer concrete with waste glass and ceramic. *Journal of Materials Research and Technology*, Vol. 23, 2023, pp. 5681–5697.
- [136] Li, Y., X. Ruan, T. Zhang, B. Fu, and H. Zeng. Case Studies in Construction Materials Durability design and construction enhancing of concrete structures in mesoscopic approach: A case

- study of a large-scale anchorage structure. *Case Studies in Construction Materials*, Vol. 19, No. August, 2023, id. e02404.
- [137] Chen, K., D. Wu, L. Xia, Q. Cai, and Z. Zhang. Geopolymer concrete durability subjected to aggressive environments – A review of influence factors and comparison with ordinary Portland cement. Construction and Building Materials, Vol. 279, 2021, id. 122496.
- [138] Pradhan, P., S. Dwibedy, M. Pradhan, S. Panda, and S. K. Panigrahi. Durability characteristics of geopolymer concrete Progress and perspectives. *Journal of Building Engineering*, Vol. 59, No. May, 2022, id. 105100.
- [139] Wasim, M., T. D. Ngo, and D. Law. A state-of-the-art review on the durability of geopolymer concrete for sustainable structures and infrastructure. *Construction and Building Materials*, Vol. 291, 2021, id. 123381.
- [140] Albitar, M., M. S. Mohamed Ali, P. Visintin, and M. Drechsler. Durability evaluation of geopolymer and conventional concretes. Construction and Building Materials, Vol. 136, 2017, pp. 374–385.
- [141] Yang, H., T. Han, W. Yang, L. Sandström, and P. G. Jönsson. Influence of the porosity and acidic properties of aluminosilicate catalysts on coke formation during the catalytic pyrolysis of lignin. *Journal of Analytical and Applied Pyrolysis*, Vol. 165, April, 2022, id. 105536.
- [142] Xie, Y., J. Xie, L. Bai, and J. Liu. Experimental study on the effect of salt on the water absorption characteristic of cement mortar. *Journal of Building Engineering*, Vol. 73, No. March, 2023, id. 106693.

- [143] Mohammed, M., A. J. A. M. Jawad, A. M. Mohammed, J. K. Oleiwi, T. Adam, A. F. Osman, et al. Challenges and advancement in water absorption of natural fiber-reinforced polymer composites. *Polymer Testing*, Vol. 124, No. March, 2023, id. 108083.
- [144] Embong, R., A. Kusbiantoro, N. Shafiq, and M. F. Nuruddin. Strength and microstructural properties of fly ash based geopolymer concrete containing high-calcium and water-absorptive aggregate. *Journal of Cleaner Production*, Vol. 112, 2016, pp. 816–822.
- [145] Reddy, P. N. and B. V. Kavyateja. Durability performance of high strength concrete incorporating supplementary cementitious materials. *Materials Today: Proceedings*, Vol. 33, 2020, pp. 66–72.
- [146] Jaji, M. B., K. A. Ibrahim, G. P. A. G. Van Zijl, and A. J. Babafemi. Effect of anisotropy on permeability index and water absorption of 3D printed metakaolin-based geopolymer concrete. *Materials Today: Proceedings*, 2023, pp. 3–8.
- [147] Hossain, M. M., M. R. Karim, M. K. Hossain, M. N. Islam, and M. F. M. Zain. Durability of mortar and concrete containing alkali-activated binder with pozzolans: A review. *Construction and Building Materials*, Vol. 93, 2015, pp. 95–109.
- [148] Bernal, S. A., R. Mejía De Gutiérrez, and J. L. Provis. Engineering and durability properties of concretes based on alkali-activated granulated blast furnace slag/metakaolin blends. *Construction* and Building Materials, Vol. 33, 2012, pp. 99–108.
- [149] Zhu, H., Z. Zhang, Y. Zhu, and L. Tian. Durability of alkali-activated fly ash concrete: Chloride penetration in pastes and mortars. Construction and Building Materials, Vol. 65, 2014, pp. 51–59.